OPTIMIZED SHAPE ADAPTIVE WAVELETS WITH REDUCED COMPUTATIONAL COST

Alfred Mertins and King N. Ngan

The University of Western Australia
EEE Dept., Nedlands 6907 WA, AUSTRALIA
mertins@ee.uwa.edu.au, king@ee.uwa.edu.au

ABSTRACT

Wavelets are often characterized through their number of vanishing moments. The more vanishing moments a wavelet has the better are the compaction properties for low-order polynomial signals. However, when bounding wavelets on intervals in order to define wavelet transforms over regions of arbitrary support, some of the moment properties get lost. This is typically accompanied with a loss of compaction gain and other unwanted effects. In this paper, we present methods for recovering the moment properties in the boundary regions. The approach recovers the moments step by step, requires a low number of computations and is well suited for the implementation with finite-precision arithmetic.

1 INTRODUCTION

The discrete wavelet transform (DWT) is known to be one of the most efficient tools for image compression [1]. The principle of this transform is to hierarchically decompose a signal into a multiresolution pyramid, where the signal is split into a coarse approximation and some detail information at each resolution level [2]. This decomposition is carried out with perfect reconstruction (PR) two-channel filter banks as shown in Figure 1. The approximation will be further decomposed in the next stage. The attractiveness of the DWT results from the fact that it provides very good compaction properties for many classes of natural images while the implementation cost is low.

Since images mainly contain low-frequency content and typically have a large DC component, it is important for compression, that the DC value of an input signal only affects the lowpass band. Moreover, it is desirable that polynomial signals of first and higher order can be represented via the lowpass component only. For signals of infinite support this is easily achieved by choosing wavelets with a sufficiently high number of vanishing moments. For example, if the wavelet $\psi(t)$ has N_ψ vanishing moments, then $\int_{-\infty}^{\infty} t^n \psi(t)dt = 0$ for $n = 0, \ldots, N_\psi - 1$. Thus, polynomial input

signals up to order $N_\psi - 1$ are represented by the lowpass band only. Similar moment properties hold for the discrete filters, which are used to carry out the DWT [2]. For example, the analysis highpass $h_1(n)$ satisfies $\sum_n n^k h_1(n) = 0$ for $k = 0, \ldots, N_\psi - 1$.
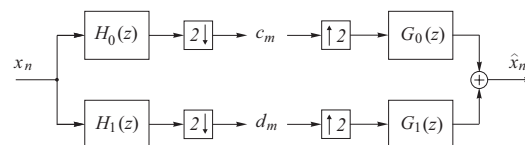
Figure 1. Two-channel filter bank.

It is important to notice that the above considerations regarding perfect reconstruction and vanishing moments only hold for infinitely sized signals. For signals of finite size, special processing steps have to be applied in the boundary regions in order to result in a support preservative transform [3, 4, 5, 6, 7, 8, 9, 10, 11, 12]. The problem of recovering moment properties in the boundary regions has been raised in [10], where boundary filters were designed in such a way that several moment conditions are satisfied by the analysis filters, resulting in wavelets that allow time-scale image analysis with low boundary distortion. For compression purposes, however, the properties of the synthesis functions are as important as those of the analysis ones. Thus, both sides should be considered jointly when designing boundary filters. This has been done in [12], where the recovery of moments was combined with the energy-normalization of the boundary filters, resulting in almost-unitary shape adaptive wavelets with arbitrary approximation order. The almost-unitary behavior is important in order to equalize the propagation of quantization errors from the subbands to the output.

In this paper, an approach to the problem of optimizing boundary filters is proposed that allows step-wise recovering of moments. The method only requires a low number of computations and can be implemented with low-precision arithmetic.

The wavelets under consideration are biorthogonal linear-phase wavelets generated from odd and even-length filters, respectively. However, the method can also be applied to non-linear phase wavelets.

2 BOUNDING WAVELETS ON INTERVALS

The wavelet transform of 2-D signals is typically carried out in a separable form, where horizontal and vertical filtering alternate. The same principle can be used for 2-D SA-DWTs, so that one mainly has to concentrate on the decomposition of arbitrary-length 1-D signals. However, the alignment of the wavelets used for the decomposition of the rows/columns is of importance. A SA-DWT should be defined in such a way that the wavelets in the interior region of an object are not affected by the actual object shape. This means that different processing schemes are needed depending on the start and stop position (even or odd) of the rows and columns.

In this paper, we concentrate on linear-phase wavelets, which are known to yield better coding results than non-linear phase ones [13]. As the initial method for a support-preservative decomposition (prior optimization), we consider symmetric extension, which already allows to maintain the DC behavior of the boundary wavelets in a simple and efficient way. Both odd and even-length linear-phase filters will be addressed.

2.1 Initial Scheme for Odd-Length Filters

Odd-length filters allow the simplest boundary processing, because symmetric reflection can be applied at any start and stop position without further modification. The principle is depicted in Figure 2(a) for a length-8 signal $x_0, x_1, \ldots, x_7$ and symmetric filters with impulse responses $\{A, B, C, B, A\}$ for the lowpass and $\{-a, b, -a\}$ for the highpass. The upper row shows the extended input signal, where the given input samples are shown in solid boxes. The lowpass and highpass subband samples, c_n and d_n, respectively, are computed by taking the inner products of the impulse responses in the displayed positions with the corresponding part of the extended input signal. Note that only four different lowpass and highpass coefficients, named as $c_0, \ldots, c_3$ and $d_0, \ldots, d_3$, occur. Only these eight different coefficients need to be stored or transmitted. At the receiver side, the subband signals can be extended accordingly, and the complete analysis/synthesis scheme is support preservative and it provides PR. A second scheme is depicted in Figure 2(b). As in Figure 2(a) we get four lowpass and four highpass coefficients, but the impulse responses have a different alignment relative to the signal. The processing of odd-length segments starting at even or odd positions is carried out by combining the schemes in Figures 2(a) and (b).

2.2 Initial Scheme for Even-Length Filters

Symmetric reflection for even-length filters is depicted in Figures 2(c) and (d). As before, decomposition schemes for odd-length segments are derived by combining the shown reflection methods. Although both schemes in Figures 2(c) and (d) are support preservative, the one in Figure 2(d) normally results in more lowpass than highpass coefficients. This can be avoided by introducing an additional highpass coefficient $d_0 = c_1 - c_0$ and neglecting c_0.

3 VANISHING BOUNDARY MOMENTS

An advantage of the symmetric extension methods described in the previous section is the continuity for DC signals. Clearly, such a signal is extended as a DC signal, so that all highpass outputs will be zero for a DC input if the highpass has zero mean.[1] This holds even in the boundary regions. Moreover, the schemes for odd-length filters in Figures 2(a) and (b) also preserve a zero of the analysis lowpass at $z = \pi$ in the boundary regions. All further moments usually do not vanish at the boundaries.

We now describe how the number of vanishing moments in the boundary regions can be increased. For this, let us consider the following matrix representation of the analysis operation (two-channel decomposition):

$$y = H\,x \qquad (1)$$

The rows of the matrix H contain the time-shifted analysis impulse responses in reversed order while the vectors x and y contain the input and the subband samples in increasing order (e.g. $y^T = [c_0, d_0, c_1, d_1, \ldots]$). In the upper left and the lower right corner of H we find the boundary filters, which are generated by folding back the original impulse responses according to the reflection schemes in Figure 2.

The operations required in order to recover some of the vanishing moments in the boundary regions may be written in the following matrix form, where v contains the new subband samples:

$$v = \begin{bmatrix} U_1 & 0 & 0 \\ 0 & I & 0 \\ 0 & 0 & U_2 \end{bmatrix} H\,x \qquad (2)$$

This means, apart from the boundaries the signal is processed as usual (indicated by the identity matrix). In the boundary regions, the impulse responses of the boundary filters are linearly combined (U_1 and U_2) in order to result in better boundary filters with more vanishing moments. Note that the inverse operation is required on the synthesis side.

---

[1] $H_1(1) = 0$ is a minimum requirement for regularity [14] and is thus assumed throughout this paper.
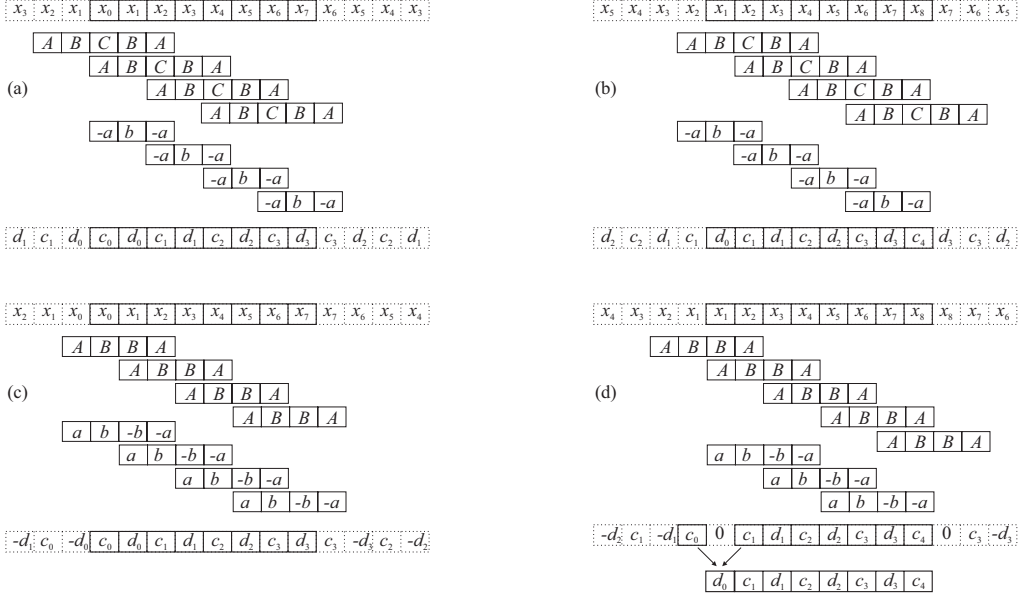
Figure 2. Symmetric reflection for even-length signals. (a) odd-length filters, segment starting at an even position; (b) odd-length filters, segment starting at an odd position. (c) even-length filters, segment starting at an even position; (d) even-length filters, segment starting at an odd position.

In order to describe a general approach to the optimization problem, let us partition v and H such that

$$v_k = U_k H_k \, x, \quad U_2 = I. \qquad (3)$$

If certain moment properties should be met by the optimized filters, the matrices U_1 and U_3 have to be restricted in a certain way. For this, let us formulate the requirements as

$$V_k = U_k \, Y_k \qquad (4)$$

where $Y_k = H_k \, [t^{(1)}, t^{(2)}, \ldots, t^{(I)}]$ contains the actual responses to specific input signals $t^{(i)}$, $i = 1, 2, \ldots, I$ and $V_k = [v_k^{(1)}, v_k^{(2)}, \ldots, v_k^{(I)}]$ contains the desired responses to these signals. For example, if we simply want to preserve the zeros of the boundary highpass filters at $\omega = 0$, which are already present due to the reflection method, we choose $V_k = Y_k = H_k \, [t^{(1)}]$ where $t^{(1)} = [1, 1, 1, 1, \ldots]^T$. If we want to add conditions on the response to linear polynomial signals, the vector $t^{(3)} = [1, 2, 3, 4, \ldots]^T$ has to be included and the desired response $v_k^{(3)}$ has to be specified.

The matrix U_k can be parameterized as follows:

$$U_k = V_k Y_k^+ + P_k Z_k^T \qquad (5)$$

where Z_k contains the basis of the nullspace of Y_k such that $Z_k^T Y_k = 0$. The matrix Y_k^+ is the pseudo inverse of Y, and P contains the free design parameters, which can be chosen in order to optimize U_k. As long as the number of conditions I is small enough to ensure that $Y_k^+ Y_k = I$, the requirements (4) are fulfilled exactly. If more conditions are added, such that $Y_k^+ Y_k \neq I$, (4)

is satisfied in the least squares sense, but there are no further free design parameters for optimization.

For extremely short segments, the boundary filters for the left and right boundary merge and H_2 vanishes. In these cases, we replace the matrices U_1 and U_3 by a common matrix U, such that $v = U H x$, where $U = V Y^+ + P Z^T$. Then, for each segment length and starting position (even or odd), a different matrix $U H$ will be implemented. The optimization of the matrices U is carried out in the same way as the optimization of U_k.

For real-time implementations of the optimized boundary filters, the above scheme with fully parameterized matrices U_1 and U_3 may be too complex. Therefore, it is of interest to describe almost optimal matrices U_k with a few sparse matrices. This can be done by first recovering the moment properties with minimal effort and then optimizing the filters by exploiting the remaining design freedom. In order to explain this, let us consider the processing of the left boundary with the scheme depicted in Figure 2(a) and let us write the standard analysis operations as

$$c_0 = h_{0,0}^T x, \quad d_0 = h_{1,0}^T x, \quad c_1 = h_{0,1}^T x, \quad \ldots$$

where $h_{0,k}^T$ and $h_{1,k}^T$ are the rows of H.

In order to recover the first vanishing moment for the first highpass filter, we may combine filters in the following way to a modified highpass:

$$f_{1,0} = h_{1,0} - \alpha(h_{0,0} - h_{0,1}) \qquad (6)$$

with

$$\alpha = \frac{h_{1,0}^T t_1}{(h_{0,0}^T - h_{0,1}^T) t_1}. \qquad (7)$$

It is easily verified that $\boldsymbol{f}_{1,0}^T \boldsymbol{t}_0 = \boldsymbol{f}_{1,0}^T \boldsymbol{t}_1 = 0$. The subtraction in (6) can be carried out prior the multiplication, which decreases the number of multiplications.

If we want also the second moment to vanish, we can add a linear combination of $(\boldsymbol{h}_{0,0} - \boldsymbol{h}_{0,1})$ and $(\boldsymbol{h}_{0,0} - \boldsymbol{h}_{0,2})$ to $\boldsymbol{h}_{1,0}$. Using this principle successively, an arbitrary number of vanishing moments can be recovered, as long as the signal length N and thus the number of available impulse responses is sufficiently high.

The operations for recovering the moment conditions may be written as operators $\boldsymbol{A}_i$

$$\boldsymbol{V}_k^{(0)} = \boldsymbol{U}_k^{(0)} \, \boldsymbol{Y}_k, \qquad (8)$$

where $\boldsymbol{U}_k^{(0)}$ has the structure

$$\boldsymbol{U}_k^{(0)} = \prod_i \boldsymbol{A}_i \qquad (9)$$

with

$$[\boldsymbol{A}_i]_{j,k} = \begin{cases} 1, & j = k \\ a_{i,k}, & j = i, k \neq i \\ 0, & \text{otherwise.} \end{cases} \qquad (10)$$

The inverses are given by

$$[\boldsymbol{A}_i^{-1}]_{j,k} = \begin{cases} 1, & j = k \\ -a_{i,k}, & j = i, k \neq i \\ 0, & \text{otherwise,} \end{cases} \qquad (11)$$

which shows that the inverse always exists. Furthermore, an implementation of quantized weights $a_{i,k}$ will cause no numerical instability.

Further optimization is carried out as follows. We first write the overall modifications to the boundary filters as

$$\boldsymbol{U}_k = [\boldsymbol{I} + \boldsymbol{P}_k \boldsymbol{Z}_k^T] \boldsymbol{U}_k^{(0)}, \qquad (12)$$

where $\boldsymbol{Z}_k$ now contains the basis of the nullspace of $\boldsymbol{U}_k^{(0)} \boldsymbol{Y}_k$ such that $\boldsymbol{Z}_k^T \boldsymbol{U}_k^{(0)} \boldsymbol{Y}_k = \boldsymbol{0}$. Then we optimize the elements of $\boldsymbol{P}_k$ with respect to an arbitrary criterion and implement the boundary processing as

$$\boldsymbol{v}^{(0)} = \boldsymbol{U}_k^{(0)} \boldsymbol{H}_k \boldsymbol{x},$$

$$\boldsymbol{v} = \boldsymbol{v}^{(0)} + \boldsymbol{P}_k [\boldsymbol{Z}_k^T \boldsymbol{v}^{(0)}]$$

The computational cost of the implementation is influenced by the choice of $\boldsymbol{Z}_k$ and by the number of non-zero entries of $\boldsymbol{P}_k$. Minimizing the cost is thus possible through choosing a sparse basis $\boldsymbol{Z}_k$. Such a sparse matrix can for instance be generated from a given $\boldsymbol{Z}_k$ by applying Givens rotations or Householder reflections. Further reduction can be achieved by implementing only those columns of $\boldsymbol{Z}_k$, which yield a significant performance improvement.

4 FILTER OPTIMIZATION

As we have seen in the last section, restoring some of the moment properties still leaves freedom of further optimization. This freedom can for example be used for optimizing the properties within a 2-D SA coding scheme. The following two points are of major importance:

1. Boundary filters operating on adjacent rows (columns) which start or stop at different positions should be well aligned in the vertical (horizontal) direction.
2. The energies of the boundary filters should be equal to the energies of the original filters which are used in the interior. Otherwise, white quantization noise may occur at the output as highly colored noise.

An objective function which includes both requirements can be stated as follows:

$$C_k(\boldsymbol{P}_k) = \lambda_1 C_k^{(1)}(\boldsymbol{P}_k) + \lambda_2 C_k^{(2)}(\boldsymbol{P}_k) \quad (13)$$
$$+ \lambda_3 \, C_k^{(3)}(\boldsymbol{P}_k)$$

with

$$C_k^{(1)}(\boldsymbol{P}_k) = \left\| \text{diag} \left\{ \boldsymbol{U}_k \boldsymbol{H}_k \boldsymbol{H}_k^T \boldsymbol{U}_k^T \right\} - \boldsymbol{1} \right\|^2$$

$$C_k^{(2)}(\boldsymbol{P}_k) = \left\| \text{diag} \left\{ (\boldsymbol{U}_k^{-1})^T \boldsymbol{G}_k^T \boldsymbol{G}_k \boldsymbol{U}_k^{-1} \right\} - \boldsymbol{1} \right\|^2$$

$$C_k^{(3)}(\boldsymbol{P}_k) = E\{\| \boldsymbol{v}_k - \boldsymbol{w}_k \|^2\}$$

Here, $\boldsymbol{1}$ is a vector containing ones, and $\text{diag}\{\cdot\}$ is a vector containing the diagonal elements of a matrix. The first term in (13) refers to the energies of the analysis boundary filters, which should be close to one. The second term states the same requirement for the synthesis side ($\boldsymbol{G}_k$ are the partitions of the synthesis operation $\boldsymbol{G} = \boldsymbol{H}^{-1}$). The third term states that the output $\boldsymbol{v}_k$ should be as close as possible to a desired output $\boldsymbol{w}_k$ where both $\boldsymbol{v}$ and $\boldsymbol{w}$ are generated from the same stochastic input. Choosing an appropriate $\boldsymbol{w}_k$ and minimizing $C_k^{(3)}(\boldsymbol{P}_k)$ allows to optimize the alignment of different boundary filters in the vertical/horizontal direction. The λ_i are arbitrary weighting factors, which allow to balance the three criteria in (13).

5 CODING RESULTS

Coding results for the cameraman image of size 256×256 are shown in Figure 3. Especially in the vicinity of sharp transitions we see that the optimized scheme does not suffer from ringing-like artifact, which occur due to coloration of the quantization noise. In this example, the 6-10 filters from [13] were used. The matrices $\boldsymbol{U}_k$ were optimized under the restriction that only the 0th moments are preserved. The matrices $\boldsymbol{Z}_k$ were chosen to allow only a subset of all possible linear combinations of lowpass and highpass filters to yield better lowpass filters and simple scale factors

<div align="center">(a)   (b)   (c)</div>
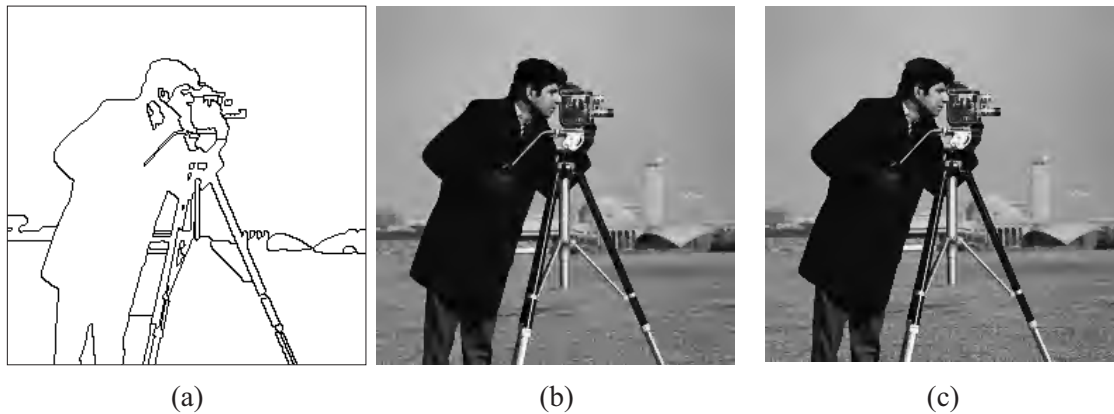
Figure 3. Coding results for the cameraman image (0.3 bpp, 6-10 filters from [13]); (a) segmentation; (b) without optimization; (c) with optimization.

for equalizing the energies of the highpass filters. The implementation cost is only one third of the cost for a full parameterization of U_k. The PSNR improvement compared to the non-optimized case is 0.6 dB and the loss compared to the full parameterization is only 0.04 dB. For odd-length filters the improvement through optimization is about 0.3 dB, while for both even and odd length filters the PSNR results are equal in the optimized case.

6 CONCLUSIONS

In this paper, we have presented methods for optimizing the boundary filters in shape adaptive wavelet transforms. Especially, we have presented a structured approach that allows to find almost-optimal solutions which require much less computations than a fully parameterized scheme, but which yield comparable coding performance.

REFERENCES

[1] M. Antonini, M. Barlaud, P. Mathieu, and I. Daubechies, "Image coding using wavelet transform," *IEEE Trans. Image Processing*, vol. 1, pp. 205–220, April 1992.

[2] S. Mallat, "A theory for multiresolution signal decomposition: The wavelet representation," *IEEE Trans. on Patt. Anal. and Mach. Intell.*, vol. 2, pp. 674–693, July 1989.

[3] J. Woods and S. O'Neil, "Subband coding of images," *IEEE Trans. Acoust., Speech, Signal Processing*, vol. 34, pp. 1278–1288, May 1986.

[4] M.J.T. Smith and S.L. Eddins, "Analysis/synthesis techniques for subband coding," *IEEE Trans. Acoust., Speech, Signal Processing*, pp. 1446–1456, Aug. 1990.

[5] H. J. Barnard, J. H. Weber, and J. Biemond, "Efficient signal extension for subband/wavelet decomposition of arbitrary length signals," in *Proc. SPIE, VCIP*, vol. 2094, pp. 966–975, November 1993.

[6] L. Chen, T. Nguyen, and K. P. Chan, "Symmetric Extension Methods for M-Channel PR LP FIR Analysis/Synthesis Systems," in *Proc. IEEE Int. Symp. Circuits and Systems*, London, UK, pp. 2.273 – 2.276, June 1994.

[7] C. Herley, "Boundary filters for finite-length signals and time-varying filter banks," *IEEE Trans. Circuits and Systems II*, vol. 42, pp. 102–114, February 1995.

[8] A. Mertins, "Time-varying and support preservative filter banks: Design of optimal transition and boundary filters via SVD," in *Proc. IEEE Int. Conf. Acoust., Speech, Signal Processing*, Detroit, USA, pp. 1316–1319, May 1995.

[9] H. J. Barnard, J. H. Weber, and J. Biemond, "A region-based discrete wavelet transform," in *Proc. European Signal Processing Conference*, pp. 1234–1237, September 1994.

[10] M. Coffrey, "Boundary compensated wavelet bases," in *Proc. IEEE Int. Conf. Acoust., Speech, Signal Processing*, München, Germany, pp. 2129–2132, May 1997.

[11] J. Apostolopoulos and J. Lim, "Transform/subband representation for signals with arbitrarily shaped regions of support," in *Proc. IEEE Int. Conf. Acoust., Speech, Signal Processing*, München, Germany, pp. 2097–2100, May 1997.

[12] A. Mertins, "Optimized biorthogonal shape adaptive wavelets," in *Proc. ICIP'98*, Chicago, October 1998.

[13] J. D. Villasenor, B. Belzer, and J. Liao, "Wavelet filter evaluation for image compression," *IEEE Trans. Image Processing*, vol. 4, pp. 1053–1060, August 1995.

[14] I. Daubechies, "Orthonormal bases of compactly supported wavelets," *Comm. Pure and Appl. Math.*, vol. XLI, pp. 909–996, 1988.